HYDRAZINE DECOMPOSITION OVER IRIDIUM SUPPORTED ON CARBON NANOFIBERS COMPOSITE FOR SPACE APPLICATIONS

Ricardo Vieira[(1)], Pierre Bernhardt[(2)], Marc-Jacques Ledoux[(2)], Cuong Pham-Huu[(2)]

[(1)]Laboratório de Combustão e Propulsão, Instituto Nacional de Pesquisas Espaciais, Rodovia Presidente Dutra Km 40, 12630-000, Cachoeira Paulista - SP, Brasil - rvieira@lcp.inpe.br
[(2)]Laboratoire des Matériaux, Surfaces et Procédés pour la Catalyse, Université Louis Pasteur, 25 rue Becquerel, 67087 Strasbourg Cedex 2, France - cuong.lcmc@ecpm.u-strasbg.fr

ABSTRACT

The aim of this work is to report the catalytic performances of iridium supported on carbon nanofiber catalyst with macroscopic shaping in the catalytic decomposition of hydrazine. The performances obtained are compared to those of the commercial catalyst Shell 405. Catalytic experiments are carried out in a 2 N microthruster placed inside a vacuum chamber in order to reproduce real-life conditions.

1. INTRODUCTION

Today most of the satellites in orbit use monopropellant hydrazine as a propulsion subsystem for orbit correction and positioning operations. The thrust is obtained by catalytic decomposition of the monopropellant on a highly loaded catalyst containing about 30 to 40 % of iridium supported on alumina. Anhydrous hydrazine decomposition initially leads to nitrogen and ammonia formations and then ammonia is further decomposed into nitrogen and hydrogen [1]. The first decomposition is a structure insensitive reaction, whereas ammonia decomposition is a structure sensitive reaction, where the large iridium particles are more active than the small ones. It is of interest to find a new catalytic system which can provide a high dispersion of the metal along with a macro- and mesoporous network in order to increase the active sites accessibility. Support with higher thermal conductivity is also needed in order to decrease hot spot formation.

Recently many authors have suggested the use of carbon nanofibers as support catalysts [3-5] due to (i) their strong metal/support interaction caused by surface prismatic planes, (ii) their high specific surface area and (iii) the absence of pores reducing the diffusion phenomena. Nevertheless, the nanometric size of the carbon nanofibers can cause reactor loading problems and pressure drop. Supporting carbon nanofibers on a macroscopic host allows the conservation of their advantages while diffusional phenomena can be avoided [6]. Carbon nanofiber composite impregnated with 30 wt. % of iridium was successfully tested in the catalytic decomposition reaction of hydrazine in a micro-pilot plant under laboratory conditions [7]. The catalytic performance in a bench scale setup is reported in the present work and compared with the commercial catalyst one.

2. EXPERIMENTAL PART

2.1. Preparation of the catalyst

The carbon felt (Carbone Lorraine Co.) with a specific surface area of 1 m^2. g^{-1} was impregnated with 1 wt. % of nickel and placed in a quartz tube located in a horizontal oven under hydrogen flow. After reduction at 400 °C for 2 h, the temperature was raised from 400 to 700 °C and hydrogen flow was replaced by the reaction mixture containing hydrogen and ethane under an appropriate molar ratio. The synthesis time was carried out at 700°C for 2 h and the carbon nanofibers yield was amounted to about 100 wt. % with respect to the initial catalyst weight [8]. The formation of carbon nanofibers significantly increases the specific surface area of the composite from 1 m^2. g^{-1} to 87 m^2. g^{-1}. The composite was cut in cylinder like forms with 7 mm o.d. and 7 mm length (Fig. 1).
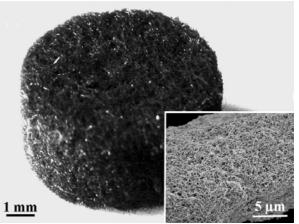

Fig. 1. Photograph of a carbon nanofiber composite. Insert: SEM image of a felt microfiber covered by carbon nanofibers.

These cylinders were impregnated with 30 wt. % of iridium using a alcoholic solution of hydrogen hexachloroiridate, and the resulting wet solid was dried at 100 °C for 2 h. The catalyst was reduced at 500 °C for 2 h followed by a thermal treatment at 500 °C during 24 h (Fig. 2). This treatment has two objectives: first, eliminate the chlorine remained in the catalyst surface and consequently decrease the mobility of the metallic particles during the fire tests [9]; second to enlarge the particle sizes and consequently increase the catalyst selectivity in hydrogen.
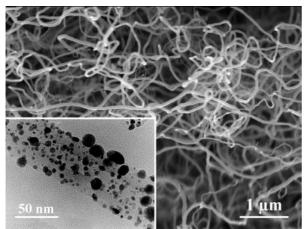
Fig 2. SEM image of carbon nanofibers. Insert: TEM image of a nanofiber covered by iridium particles

2.2. Test conditions

The catalysts were tested in a bench scale fire test (Fig. 3) constituted by a vacuum chamber simulating the pressure conditions in the space and an acquisition data system.
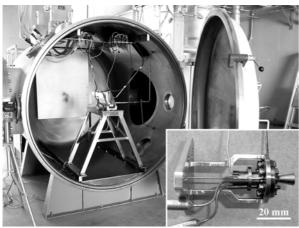

Fig. 3. Photograph of the vacuum chamber of the Test Bench of the INPE. Insert: 2 N microthruster used during the tests.

Table 1. Operating conditions of propellant valve. Propellant pressure injection (P_{inj}), pulse-on (t_{on}) and pulse-off (t_{off}) modes.

Test	$P_{inj.}$ (bar)	t_{on} (ms)	t_{off} (ms)
1	5,5	20	980
2	5,5	100	900
3	5,5	200	800
4	5,5	500	500
5	5,5	5000	-
6	22	20	980
7	22	100	900
8	22	200	800
9	22	500	500
10	22	5000	-

The tests were carried in a 2 N microthruster projected to operate with the commercial catalyst Shell 405.
The tests were carried out under two hydrazine injection pressures, i. e., 22 and 5.5 bar, simulating the real conditions of the propellant reservoir pressure at the beginning and the end of the satellite life, respectively. For each pressure 4 series of 100 short pulses and 1 duty cycle were performed (Table 1). The catalyst bed was pre-heated at 120 °C for all tests.

2.3. Performance evaluations

The parameters of performance evaluations of the different catalysts in the microthruster adopted were: the steady-state thrust, the chamber pressure variations and the ignition time delay, the latter one being defined as the time response from valve signal to 90 % of steady-state chamber pressure .

3. RESULTS AND DISCUSSION

The dimensions of the microthruster reaction chamber are 6.7 mm diameter for 20 mm length. The microthruster was loaded with 1.14 g of the reference catalyst and with 0.15 g of the carbon nanofiber based catalyst. Table 2 shows the thrust average values of series of 100 pulses in different conditions of hydrazine injection.

Table 2. Average thrust (F) values of the catalysts performances in N and the temperature of reaction chamber (Tc) in °C from some series of 100 pulses under different propellant feed pressure and pulse widths.

	$P_{inj.}$ (bar)	t_{on} 20/t_{off} 980		t_{on} 200/t_{off} 800		t_{on} 500/t_{off} 500	
		F	T_c	F	T_c	F	T_c
Shell	5.5	0.34	380	0.63	610	0.66	680
Ir/NFC	5.5	0.40	340	0.85	610	0.75	660
Shell	22	0.44	440	2.25	730	2.25	780
Ir/NFC	22	1.20	420	2.65	560	2.20	640

The carbon nanofiber based catalyst showed superior thrust (F) performances than the reference catalyst. These better performances can be explained by the large metallic surface exposed on the carbon nanofiber based catalyst, despite the mass introduced in the microthruster which is ten times lower than the quantity used with the commercial catalyst. This performance can also be attributed to high external surface area of the support which provides a high accessibility to the reactant. In this type of reaction, where the heat and mass transfers must be very fast, the reactant does not have time to penetrate into the pores and the main reaction occurs on the external surface of

the catalyst grains. This can be confirmed by the increase of the performance of the Shell 405 in relation to the Ir/NFC tested at 22 bar. The feed pressure increase allows the propellant to penetrate deeply inside the pores of the reference catalyst and, as a consequence, significantly increases the decomposition rate. The temperature values (Tc) showed in Table 2 represent the maximum values measured on the external wall of the microthruster during each test of 100 consecutive pulses. The lower temperature value observed on the Ir/NFC catalyst compared to the one observed on the reference catalyst is due to a better thermal conductivity on carbon than on alumina, leading to a better evacuation of the heat generated during the decomposition reaction.
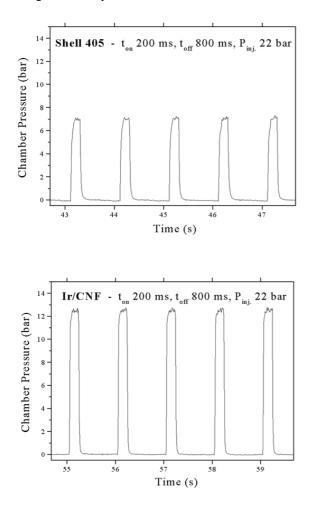

Fig. 4. Part of a chamber pressure curve of the Shell 405 (on top) and Ir/NFC (below) catalysts during a series of 100 pulses t_{on} 200 ms and t_{off} 800 ms.

Figure 4 shows the evolution of the pressure generated in the reaction chamber during the hydrazine decomposition. Both catalysts did not show instability ranges superior 10 % and spikings superior 50 % of the stagnation pressure.

The pressure response time is considered as the time required to reach 90 % of the steady-state chamber pressure. The Ir/NFC and Shell 405 catalysts showed an ignition delay of 46 ms and 62 ms at 5.5 bar respectively. In the tests at 22 bar, both catalysts presented similar performances, the ignition delay were 41 ms and 43 ms for the Ir/NFC and Shell 405 catalysts. In the lower pressure level, the carbon nanofiber catalyst has a more spontaneous restarted capability than the Shell 405. The performance of the Shell catalyst increases with the propellant injection pressure due to better penetration of the propellant in the pores of the catalyst, allowing the active sites, located in the interior of the pores, to participate to the reaction.

4. CONCLUSION

The results show that the decomposition reaction of hydrazine iridium catalyst deposited on carbon nanofiber composite has a better performance than commercial catalyst supported on alumina. This better performance is attributed to the high external surface area of carbon nanofibrers, that facilitates the monopropellant diffusion into the catalyst. Moreover the high thermal conductivity of the carbon based support allows a fast homogenization of the heat generated during the reaction throughout the catalyst body, preventing the formation of hot spots which are detrimental to the active phase and catalyst body conservation. Finally, the carbon nanofibers composite can also be used efficiently as catalytic support in liquid phase reactions where diffusional phenomena of the reactants are essential and in reactions which present high mass and heat transfers.

5. REFERENCES

1. Schimidt, H. D. *Hydrazine and its derivatives. Preparation, Properties and Applications*, John Wiley: N.Y. 1984.
2. Balcon, S. *PhD. Thesis*, Université de Poitiers, France, 1996.
3. Rodriguez, N.M.; Kim, M.S. Baker, R. T. K. *J. Phys. Chem.*, 98, 108, 1994.
4. Salman, F.; Park, C. Baker, R. T. K. *Catal. Today*, 53, 385, 1999.
5. Pham-Huu, C.; Keller, N.; Charbonniére, R.; Ziessel, R. Ledoux, M.J. *Chem. Commun.*, 1871, 2000.
6. Pham-Huu, C.; Vieira, R.; Charbonnière, L.; Ziessel, R. Ledoux, M. J. *French Pat.* 0115178, 2001.
7. Vieira, R.; Pham-Huu, C.; Keller, N. Ledoux, M. J. *Chem. Commun.,* 954, 2002.
8. Vieira, R.; Pham-Huu, C.; Keller, N. Ledoux, M. J. *Quim. Nova*, 26, 665, 2003.
9. Balcon, S.; Mary, S.; Kappenstein, C. Gengembre, E. *Appl. Catal.,* 196, 179, 2000.